

Transmission-electron-microscopy study of charge-stripe order in $\text{La}_{1.725}\text{Sr}_{0.275}\text{NiO}_4$

Jianqi Li, Yimei Zhu, and J. M. Tranquada
Brookhaven National Laboratory, Upton, NY 11973-5000

K. Yamada
Institute for Chemical Research, Kyoto University, Gokashou, Uji, 611-0011 Kyoto, Japan

D. J. Buttrey
Department of Chemical Engineering, University of Delaware, Newark, Delaware 19716
 (Dated: November 6, 2018)

We characterize the local structure and correlations of charge stripes in $\text{La}_{1.725}\text{Sr}_{0.275}\text{NiO}_4$ using transmission-electron microscopy. We present direct evidence that the stripe modulation is indeed one-dimensional within each NiO_2 plane. Furthermore, we show that individual stripes tend to be either site-centered or bond-centered, with a bias towards the former. The spacing between stripes often fluctuates about the mean, contributing to a certain degree of frustration of the approximate body-centered stacking along the c -axis. These results confirm ideas inferred from previous neutron-diffraction measurements on doped nickelates, and demonstrate that charge-stripe order is quite different from the conventional concept of charge-density-wave order.

The tendency in hole-doped two-dimensional antiferromagnets for charges to order in stripes is an empirically established phenomenon that is of particular interest for its possible relevance to superconductivity in the cuprates.^{1,2} Despite considerable progress on the experimental front, the theoretical identification of the dominant effects responsible for the occurrence of stripe correlations remains controversial.^{3,4,5,6,7,8,9,10,11,12,13} For superconducting cuprates, where the stripes are oriented parallel to the Cu-O bonds, there is considerable theoretical interest in whether the stripes tend to be centered on rows of Cu atoms (site-centered stripes) or on rows of O atoms (bond-centered).^{9,11} In the case of nickelates, the stripes run diagonally, at 45° to the Ni-O bonds, and information on the lattice alignment of the stripes has been inferred from neutron diffraction studies.¹⁴ From measurements on $\text{La}_2\text{NiO}_{4.133}$ it has been inferred that there is a temperature-dependent shift from mostly site-centered stripes at low temperature to all bond-centered stripes above the spin-ordering temperature.^{14,15} It is desirable to test such inferences with local, real-space images, and to test their generality in Sr-doped nickelates, which lack the long-range stripe order of $\text{La}_2\text{NiO}_{4.133}$.

In this paper we report a transmission-electron-microscopy (TEM) study of charge stripes in $\text{La}_{1.725}\text{Sr}_{0.275}\text{NiO}_4$, a composition that has been characterized previously by neutron scattering.^{16,17} Though not the composition with the longest correlation length,¹⁸ the incommensurability of the charge stripe order makes it an interesting test case. From the neutron work,¹⁷ it is known that the charge ordering temperature of this sample is ~ 190 K. Here we present the first direct evidence, to our knowledge, that the charge-order modulation in nickelates is truly one-dimensional. We also present lattice images sensitive to the stripes, demonstrating that they frequently exhibit irregular spacing and that they have a tendency to be either site- or bond-centered, with a bias towards site-centered in

this sample at low temperature.

There have been a number of TEM studies of nickelates, with most^{19,20,21,22} focussed on determination of the interstitial order in $\text{La}_2\text{NiO}_{4+\delta}$. We actually spent considerable time trying to characterize $\text{La}_2\text{NiO}_{4.133}$, and saw some of the modulations reported previously^{19,20,21,22}; however, these ordering wave vectors are not all consistent with what has been observed by neutron diffraction on large crystals.²³ We suspect that the lack of consistency between neutron and electron diffraction measurements is associated with the mobility of the oxygen interstitials, as suggested by Otero-Diaz and coworkers.²⁰ In part due to these difficulties, we turned to $\text{La}_{2-x}\text{Sr}_x\text{NiO}_4$, the system in which charge ordering was first discovered.²⁴

Starting with a piece of the $\text{La}_{1.725}\text{Sr}_{0.275}\text{NiO}_4$ single crystal used in the neutron study,¹⁷ specimens for TEM observations were prepared by mechanical polishing to a thickness of around $10\text{ }\mu\text{m}$, followed by ion milling. In addition, we also prepared some thin samples for electron diffraction experiments simply by crushing the bulk material into fine fragments, which were then supported by a copper grid coated with a thin carbon film. The TEM investigations were performed on a JEOL-3000F (300 kV) field-emission electron microscope equipped with an energy filter. All of the measurements reported here were performed with the sample holder cooled by liquid nitrogen, giving an approximate sample temperature of 86 K. Images were recorded on either image plates or a CCD (charge-coupled device) camera. Although the average crystal structure is tetragonal (space group $I4/mmm$), it is convenient to index the Bragg reflections with an $F4/mmm$ unit cell, such that $a = b = 5.4\text{ }\text{\AA} = 2\sqrt{2}d_{\text{Ni-O}}$, with $c = 12.6\text{ }\text{\AA}$.

Figures 1(a) and (b) display the low-temperature diffraction patterns taken along the $[001]$ and $[010]$ zone-axis directions, respectively. Both diffraction patterns show notable superlattice reflections in addition to the

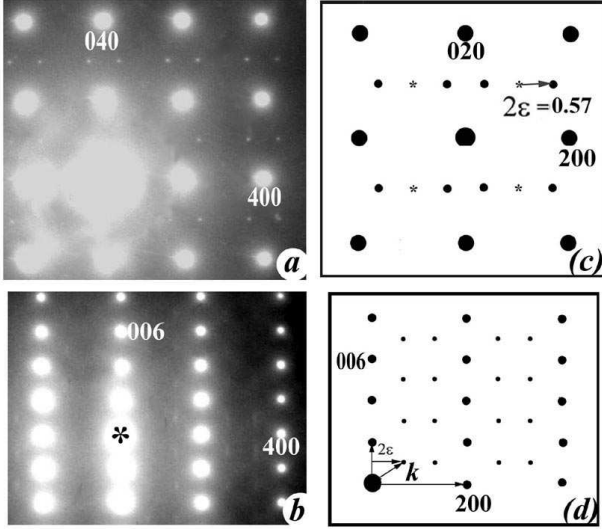


FIG. 1: Electron diffraction patterns taken along (a) [001] and (b) [010] zone-axes, showing the presence of superlattice spots at 86 K. Schematic illustrations identify the satellite spots in the reciprocal lattice planes (c) a^*-b^* and (d) a^*-c^* .

fundamental Bragg diffraction spots. Schematic representations of the diffraction patterns, corresponding to the a^*-b^* and a^*-c^* planes of reciprocal space, are shown in Figs. 1(c) and (d), respectively. The superstructure peaks are characterized by a unique modulation wave vector, $\mathbf{k} = (2\varepsilon, 0, 1)$, with $2\varepsilon \approx 0.57$, corresponding to $\varepsilon \approx 0.285$, a value consistent with the neutron work.¹⁷ Note that a more typical [001]-zone-axis pattern, as shown in Fig. 2(a), exhibits a second modulation wave vector, $\mathbf{k}' = (0, 2\varepsilon, 1)$ (see also Ref. 24). The presence of a single modulation wave vector in Fig. 1(a) is clear evidence that the stripe modulation within an NiO_2 layer is one-dimensional. The occurrence of both \mathbf{k} and \mathbf{k}' in Fig. 2(a) is due to the presence of distinct stripe domains rotated by 90° to one another. Such twinning is expected, since the tetragonal lattice provides no unique orientation for the stripe modulation.

To further characterize the structural modulation, we have made a comprehensive examination along several relevant orientations and in many areas of the sample over the temperature range of 300 K down to 86 K. Generally, the superstructure reflections look very weak and only become detectable as the temperature is reduced below 200 K, the approximate charge-ordering temperature.¹⁷ The superlattice spots on the a^*-b^* plane are very sharp, indicating a relatively long coherence length of the ordered state within the NiO_2 planes. The diffraction pattern along the [010] zone axis exhibits weak diffuse spots that are extended along the c^* direction, indicating a short correlation length along the c -axis, perpendicular to the NiO_2 planes. The incommensurability ε is observed to vary slightly from one area to another within the range of 0.28–0.3; similar variations were ob-

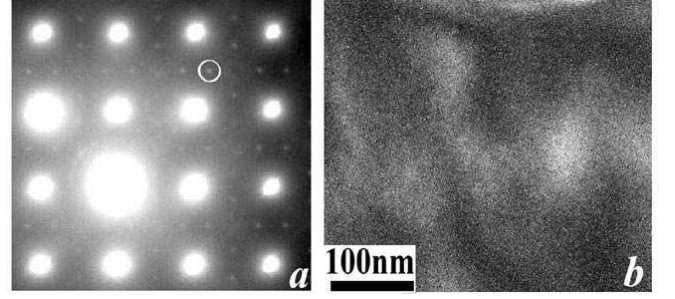


FIG. 2: (a) Electron diffraction pattern taken from an area showing 90° -twinning of superlattice modulations. (b) Dark-field image produced by a satellite spot, circled in (a), at the temperature of 86 K, illustrating the complex charge-ordered domains in the a - b plane.

served previously.²⁴

Let us return to Fig. 2(a) and its orthogonal sets of superstructure diffraction spots along the a^* and b^* directions. We can test our assertion that these spots are distinct twin domains by forming a dark-field TEM image using the circled satellite peak. If the two sets of peaks came from the same domain, then we would expect the intensity of the dark-field image to be uniform. Instead, the actual image, Fig. 2(b), shows a complex domain-like contrast. The bright regions represent domains that contribute to the superlattice peak. The dark regions are associated with the orthogonal domains. From the size of the bright domains, one can estimate a typical domain size of ~ 50 nm.

The dark-field images of the charge-ordered state within the a - c crystalline plane have also been checked in many areas at low temperature. As mentioned above, the superlattice spots generally are weak and diffuse along the direction of the c^* -axis as shown in Fig. 1(b). We further illustrate these features in Fig. 3(a). The weak, diffuse nature of the spots makes the measurements of dark-field images at low temperatures quite challenging. A very long exposure time is required to obtain a utilizable dark-field image, and less-than-perfect mechanical stability of the sample during such an exposure results in low spatial resolution. Figure 3(b) shows a dark-field image taken with the superlattice reflection circled in Fig. 3(a). Despite the weak contrast, this image reveals the presence of complex domain structure. In order to better depict the structural properties of the charge ordered state, we have smoothed the image and created a two-level contour map, shown in Fig. 3(c) illustrating the domain configuration within the examined area. This contour map indicates more clearly the domain features present in Fig. 3(b). As one can see, domains tend to be elongated along the a -axis. Close examination of these charge order domains suggests that the longitudinal dimension varies from 10–80 nm. The transverse dimension, along the c -axis, is much smaller, ranging from 2–5 nm. The dimensions and orientation of the domains are

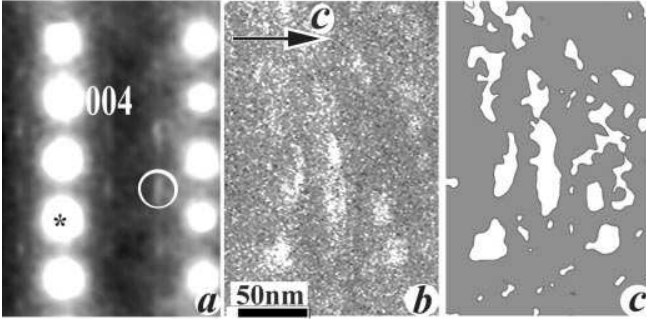


FIG. 3: (a) [010] zone-axis diffraction pattern showing the diffuse superlattice reflections in the a^*-c^* plane at 86 K. (b) Dark-field image obtained from the circled satellite spot. The corresponding CO domains are the bright regions. (c) A smoothed, two-level contour-map version of (b) to emphasize the charge domains in the examined area.

consistent with the shape of the superlattice reflections.

To study the local ordering of the charge stripes with respect to the lattice, we turn to high-resolution TEM images. The images shown in Figs. 4–6 involve projections along the [010] axis that were obtained from thin regions of the sample utilizing the Scherzer defocus condition. Under these circumstances, the projected rows of heavier atoms, such as La and Ni, appear as dark spots; their positions are indicated in Fig. 4(a). Following this identification, it is clear that the bright spots within each NiO_2 plane are associated with the O rows. The modulation of the contrast at the O sites should result from a combination of charge and structural modulations. To properly correlate the brighter and darker O spots with hole rich and poor regions requires a detailed image simulation. Such a simulation is challenging because of the need to model both atomic displacements and charge modulation. In the absence of a suitable simulation, we simply note below that associating the brighter O spots with hole-rich columns yields a satisfying consistency with simple models.

Figure 4(a) shows an image in which the charge stripes, viewed edge on, appear to be dominantly centered on Ni rows, as indicated by bright pairs of spots. The intensity profile along a line through the bottom NiO_2 layer is presented in Fig. 4(b). The Ni rows correspond to local minima in the contrast, and the O rows to local maxima. A corresponding schematic model for the charge and spin stripes (involving only the Ni sites) is shown in Fig. 4(c).

There are also regions of the sample that appear to exhibit alternating O-centered and Ni-centered stripes; one of these is shown in Fig. 5(b). We associate O-centered stripes with the occurrence of three bright spot in a row, with the center one being the brightest. Figure 5(a) shows a model for equally-spaced, alternating site- and bond-centered stripes within an NiO_2 plane. Such a configuration corresponds to $2\varepsilon = 2/3.5$, or $\varepsilon = 0.286$, very close to the average value determined by electron diffraction. To obtain the same period with only Ni-centered

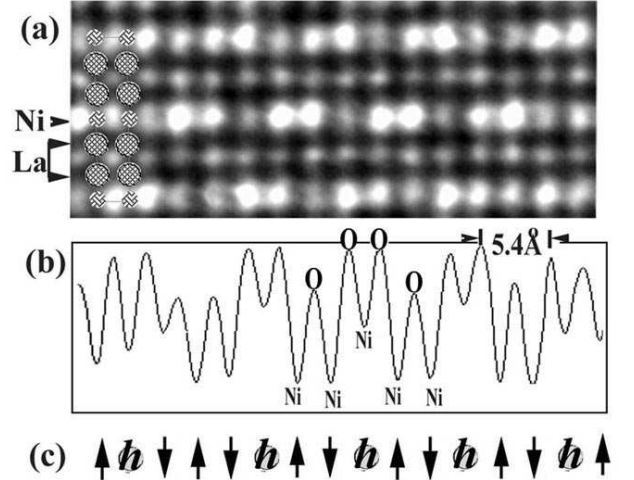


FIG. 4: (a) High-resolution TEM image of the a - c plane (c vertical) illustrating the modulation at low temperature. The bright segments arising from charge modulation within the NiO_2 layers can be recognized. (b) An intensity profile showing contrast variation within the bottom NiO_2 layer of (a). This curve clearly indicates that the brighter segments in this region are Ni-centered. (c) Schematic model of spin and charge ordering corresponding to the curve in (b).

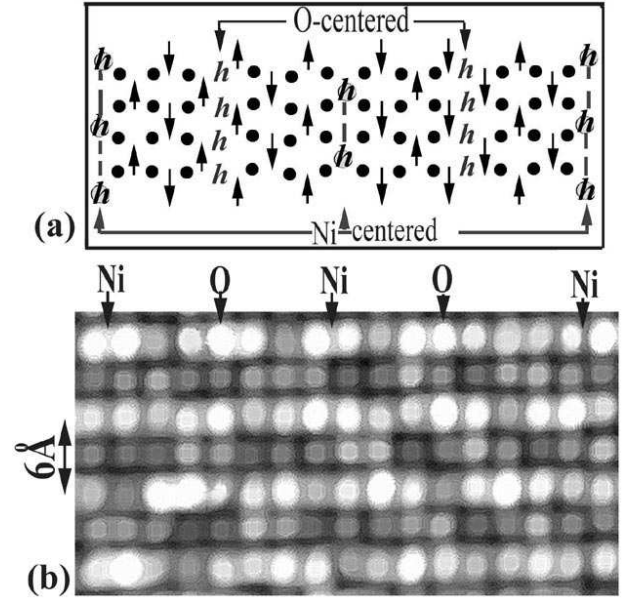


FIG. 5: (a) Schematic model of alternating Ni- and O-centered stripes within an NiO_2 plane. This configuration corresponds to $\varepsilon = 0.286$. (Note that the hole density is not properly represented in the O-centered stripes.) (b) High-resolution TEM image of the a - c plane (c vertical) demonstrating the appearance of alternating O-centered and Ni-centered charge stripes along the modulation direction. The centers of the charge stripes in the top row are labelled. Note that only the first two on the left are aligned with the charge stripes indicated in (a).

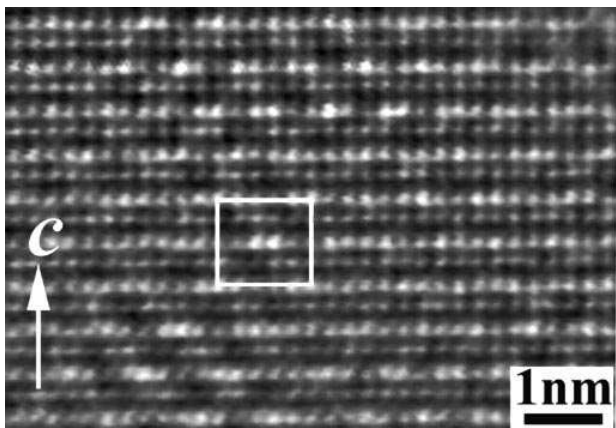


FIG. 6: High-resolution TEM image showing a larger area in the a - c plane. The relative ordering of the charge stripes along the c -axis direction can be seen. The white box outlines an approximate unit cell.

stripes requires alternating stripe spacings of $1.5a$ and $2a$, as discussed in Ref. 14. (Note that there are two Ni rows per orthorhombic unit cell.) Irregular spacing is apparent in all rows, including the first.

The last issue to be discussed is the stacking of stripes from one layer to the next. Figure 6 shows another image of the a - c plane, but with lower magnification. Despite plenty of defects, one can observe many stripes within the layers and their tendency to form a body-centered stacking along the c -axis. Such an arrangement minimizes the Coulomb repulsion between the stripes. The white box outlines an approximate unit cell. The body-centering is only approximate because of the pinning of the stripes to the lattice. This is especially apparent in Fig. 4(a), where, in moving from one layer to the next, the Ni-centered stripes can shift only by increments of $a/2$. For this sample, with an average stripe spacing of

about $1.75a$, it is not possible to have a perfectly body-centered stacking as long as the stripes are pinned to the lattice. This conclusion was first reached in a neutron diffraction study,¹⁴ and the high-resolution TEM images provide solid confirmation of it. Finally, we note that the body-centered stacking makes it impossible to image the stripes directly in the a - b plane, as a projection along the c -axis will average out all stripe contrast.

In summary, we have presented a systematic TEM investigation of superlattice modulation in $\text{La}_{1.725}\text{Sr}_{0.275}\text{NiO}_4$ at low temperature. The observation of sample regions with a single modulation wave vector provides direct evidence that the stripe modulation is indeed one-dimensional, and not grid-like. This conclusion is also supported by dark-field images formed from individual superlattice reflections. A similar conclusion regarding diagonal spin stripes in $\text{La}_{2-x}\text{Sr}_x\text{CuO}_4$ with $x \lesssim 0.055$ has been obtained by neutron diffraction²⁵; in that case, the stripe orientation is tied to the orthorhombic symmetry of the lattice, which contrasts with the tetragonal symmetry of our nickelate sample. Close examination of the high-resolution TEM images suggests that the charge stripes are predominantly centered on rows of Ni atoms, although alternative mixtures of Ni- and O-centered stripes also appear in some small regions.

Research at Brookhaven is supported by the Department of Energy's (DOE) Office of Science under Contract No. DE-AC02-98CH10886. KY acknowledges support from the Japan Science and Technology Corporation, the Core Research for Evolutional Science and Technology Project (CREST), and Grants-in-Aid for Scientific Research on Priority Areas, 12046239, 2001 and Research (A), 10304026, 2001 and for Creative Scientific Research (13NP0201) from the Japanese Ministry of Education, Culture, Sports, Science, and Technology. DJB acknowledges support from DOE under Contract No. DE-FG02-00ER45800.

- ¹ J. Orenstein and A. J. Millis, *Science* **288**, 468 (2000).
- ² V. J. Emery, S. A. Kivelson, and J. M. Tranquada, *Proc. Natl. Acad. Sci. USA* **96**, 8814 (1999).
- ³ J. Zaanen and O. Gunnarsson, *Phys. Rev. B* **40**, 7391 (1989).
- ⁴ M. Kato, K. Machida, H. Nakanishi, and M. Fujita, *J. Phys. Soc. Jpn.* **59**, 1047 (1990).
- ⁵ J. Zaanen and P. B. Littlewood, *Phys. Rev. B* **50**, 7222 (1994).
- ⁶ U. Löw, V. J. Emery, K. Fabricius, and S. A. Kivelson, *Phys. Rev. Lett.* **72**, 1918 (1994).
- ⁷ C. Castellani, C. Di Castro, and M. Grilli, *Phys. Rev. Lett.* **75**, 4650 (1995).
- ⁸ C. Nayak and F. Wilczek, *Phys. Rev. Lett.* **78**, 2465 (1997).
- ⁹ S. R. White and D. J. Scalapino, *Phys. Rev. Lett.* **80**, 1272 (1998).
- ¹⁰ C. S. Hellberg and E. Manousakis, *Phys. Rev. Lett.* **83**, 132 (1999).
- ¹¹ M. Vojta and S. Sachdev, *Phys. Rev. Lett.* **83**, 3916 (1999).
- ¹² D. I. Khomskii and K. I. Kugel, *Europhys. Lett.* **55**, 208 (2001).
- ¹³ D. Podolsky, E. Demler, K. Damle, and B. I. Halperin, *cond-mat/0204011*.
- ¹⁴ P. Wochner, J. M. Tranquada, D. J. Buttrey, and V. Sachan, *Phys. Rev. B* **57**, 1066 (1998).
- ¹⁵ J. M. Tranquada, P. Wochner, A. R. Moodenbaugh, and D. J. Buttrey, *Phys. Rev. B* **55**, R6113 (1997).
- ¹⁶ S.-H. Lee, S.-W. Cheong, K. Yamada, and C. F. Majkrzak, *Phys. Rev. B* **63**, 060405 (2001).
- ¹⁷ S.-H. Lee, J. M. Tranquada, K. Yamada, D. J. Buttrey, Q. Li, and S.-W. Cheong, *Phys. Rev. Lett.* **88**, 126401 (2002).
- ¹⁸ H. Yoshizawa, T. Kakeshita, R. Kajimoto, T. Tanabe, T. Katsufuji, and Y. Tokura, *Phys. Rev. B* **61**, R854 (2000).
- ¹⁹ Z. Hiroi, T. Obata, M. Takano, Y. Bando, Y. Takeda, and

- O. Yamamoto, Phys. Rev. B **41**, 11665 (1990).
- ²⁰ L. C. Otero-Diaz, A. R. Landa, F. Fernandez, R. Saez-Puche, R. Withers, and B. G. Hyde, J. Solid State Chem. **97**, 443 (1992).
- ²¹ A. Demourgues, F. Weill, J. C. Grenier, A. Wattiaux, and M. Pouchard, Physica C **109**, 425 (1992).
- ²² M. J. Sayagués, M. Vallet-Regí, J. L. Hutchison, and J. M. González-Calbet, J. Solid State Chem. **125**, 133 (1996).
- ²³ J. M. Tranquada, J. E. Lorenzo, D. J. Buttrey, and V. Sachan, Phys. Rev. B **52**, 3581 (1995).
- ²⁴ C. H. Chen, S.-W. Cheong, and A. S. Cooper, Phys. Rev. Lett. **71**, 2461 (1993).
- ²⁵ S. Wakimoto, R. J. Birgeneau, M. A. Kastner, Y. S. Lee, R. Erwin, P. M. Gehring, S. H. Lee, M. Fujita, K. Yamada, Y. Endoh, et al., Phys. Rev. B **61**, 3699 (2000).